View metadata, citation and similar papers at core.ac.uk
brought to you by CORE
provided by Elsevier - Publisher Connector

Neuron 52, 663–677, November 22, 2006 ©2006 Elsevier Inc. DOI 10.1016/j.neuron.2006.09.029

Mechanisms Underlying the Rapid Induction and Sustained Expression of Synaptic Homeostasis

C. Andrew Frank,[1,2] Matthew J. Kennedy,[1,2] Carleton P. Goold,[1] Kurt W. Marek,[1] and Graeme W. Davis[1,*]
[1] Department of Biochemistry and Biophysics
Neuroscience Program
University of California, San Francisco
1550 4th Street, Rock Hall 4th Floor North
San Francisco, California 94158

Summary

Homeostatic signaling systems are thought to interface with the mechanisms of neural plasticity to achieve stable yet flexible neural circuitry. However, the time course, molecular design, and implementation of homeostatic signaling remain poorly defined. Here we demonstrate that a homeostatic increase in presynaptic neurotransmitter release can be induced within minutes following postsynaptic glutamate receptor blockade. The rapid induction of synaptic homeostasis is independent of new protein synthesis and does not require evoked neurotransmission, indicating that a change in the efficacy of spontaneous quantal release events is sufficient to trigger the induction of synaptic homeostasis. Finally, both the rapid induction and the sustained expression of synaptic homeostasis are blocked by mutations that disrupt the pore-forming subunit of the presynaptic $Ca_V2.1$ calcium channel encoded by *cacophony*. These data confirm the presynaptic expression of synaptic homeostasis and implicate presynaptic $Ca_V2.1$ in a homeostatic retrograde signaling system.

Introduction

Homeostasis is an essential type of feedback regulation that enables a biological system to maintain a constant functionality within a changing environment. In the nervous system, homeostatic signaling systems have been implicated in the control of both nerve and muscle excitability (Davis, 2006; Davis and Bezprozvanny, 2001; Marder and Prinz, 2002; Perez-Otano and Ehlers, 2005; Turrigiano and Nelson, 2004). In the central nervous system, homeostatic signaling systems have been shown to counteract chronic perturbations of neuronal excitation though modulation of ion channel density and neurotransmitter receptor abundance (Beattie et al., 2002; Murthy et al., 2001; Thiagarajan et al., 2005; Turrigiano et al., 1994, 1998). In the peripheral nervous system, homeostatic control of synaptic efficacy has been documented at the neuromuscular junction (NMJ) of organisms including *Drosophila*, rodent, and human (Davis and Bezprozvanny, 2001; Davis et al., 1998; Petersen et al., 1997; Plomp et al., 1994). At the NMJ, mutations that decrease the sensitivity of postsynaptic neurotransmitter receptors lead to a compensatory, homeostatic increase in synaptic efficacy. The increase in synaptic efficacy precisely offsets the perturbation of postsynaptic receptor function and leads to normal muscle excitation (Davis et al., 1998; DiAntonio et al., 1999; Petersen et al., 1997; Plomp et al., 1992).

It is generally believed that homeostatic signaling at the neuromuscular junction is slow, being induced and expressed over a period of several hours to days (Davis and Bezprozvanny, 2001; Davis and Goodman, 1998; Petersen et al., 1997; Plomp et al., 1992). This model is thought to reflect the time over which muscle activity is integrated by the homeostatic signaling system (Davis and Bezprozvanny, 2001; Turrigiano and Nelson, 2004). Consistently, it is believed that the mechanisms of homeostatic compensation may be directly linked to the slow, developmental growth of the NMJ (Davis and Bezprozvanny, 2001; Davis and Goodman, 1998; Turrigiano and Nelson, 2004). However, since prior experiments have exclusively utilized manipulations that persist for several days of development, it has not been possible to test the time course or molecular mechanisms that are responsible for the induction of synaptic homeostasis.

Many additional questions remain. For example, homeostatic signaling implies the existence of mechanisms that monitor nerve or muscle activity and integrate this information over time (Davis and Bezprozvanny, 2001; Davis, 2006; Marder and Prinz, 2002). The molecular identity of an activity "monitor" and the time over which neural activity is integrated to achieve homeostatic compensation remain unknown both centrally and peripherally, though postsynaptic calcium and CamKII signaling are thought to be involved (Haghighi et al., 2003; Thiagarajan et al., 2002; Turrigiano et al., 1994). Homeostatic modulation of synaptic efficacy at the NMJ, and possibly central synapses, could involve the modulation of presynaptic neurotransmitter release (Murthy et al., 2001; Piedras-Renteria et al., 2004). This implies the existence of a retrograde signaling system. The identity of this retrograde signal and the identity of the presynaptic effector proteins that mediate altered neurotransmission also remain generally unknown.

Here we demonstrate that homeostatic signaling at the *Drosophila* NMJ can potentiate presynaptic transmitter release within 5–10 min following pharmacological blockade of postsynaptic neurotransmitter receptors. Therefore, changes in muscle activity must be integrated by the homeostatic system over a period of seconds to minutes, a process that is far more rapid than previously demonstrated at the NMJ (Plomp et al., 1992) or central synapses (Murthy et al., 2001; Sutton et al., 2006; Sutton and Schuman, 2005; Thiagarajan et al., 2005; Turrigiano and Nelson, 2004). We then demonstrate that the rapid induction of synaptic homeostasis occurs in the absence of motoneuron activity and, therefore, does not require evoked neurotransmission. These data suggest that the altered efficacy of spontaneous miniature release events that persist in

*Correspondence: gdavis@biochem.ucsf.edu
[2] These authors contributed equally to this work.

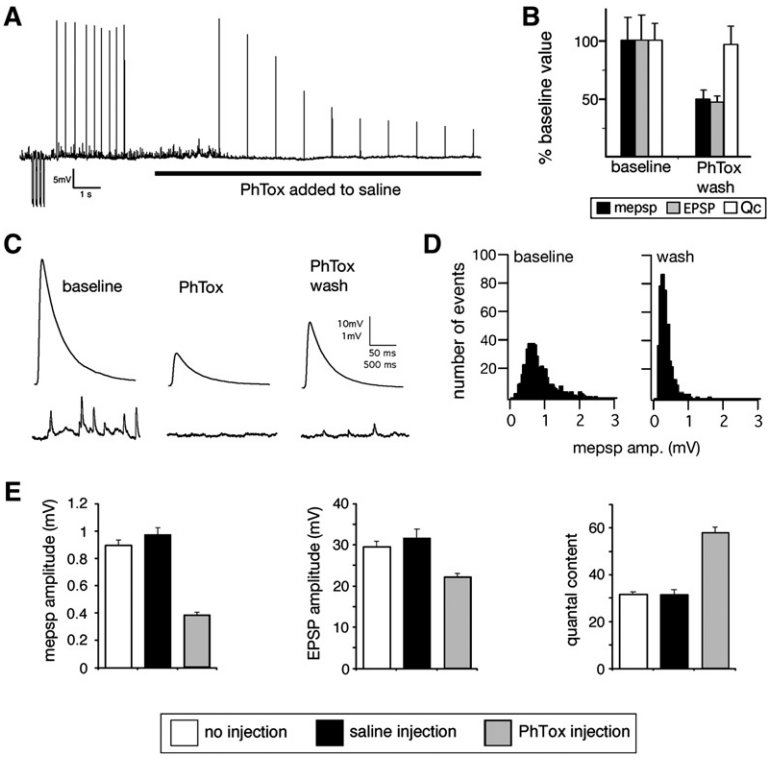

Figure 1. Rapid Induction of Synaptic Homeostasis following Injection of a Glutamate Receptor Antagonist

(A) Sample recording from the NMJ showing a stimulus-dependent decline in mEPSP and EPSP amplitudes following PhTox bath application (horizontal line).

(B) Average mEPSP, EPSP amplitudes, and quantal content (Qc) prior to PhTox application (baseline; n = 12) and following a 2 min PhTox incubation with 30 s washout (PhTox-wash; n = 13). Recording saline lacks PhTox.

(C) Sample traces for the data presented in (B).

(D) Histograms reveal that the mEPSP amplitude distribution is shifted toward smaller values following PhTox application and washout (right graph; wash). Samples sizes are equivalent.

(E) Quantification of average mEPSP amplitude (graph at left), average EPSP amplitude (middle graph), and quantal content (graph at right). Quantification was performed for three conditions, including 30 min after 200 μM PhTox injection (PhTox injection; n = 30), 30 min after saline injection (saline injection; n = 17), versus uninjected controls (no injection, n = 10). There is a significant homeostatic increase in quantal content in the PhTox-injected animals compared to controls ($p < 0.001$).

Error bars represent SEM.

the absence of motoneuron activity is sufficient to induce rapid homeostatic signaling at the NMJ. Finally, we demonstrate that mutations in the pore-forming subunit of an essential presynaptic calcium channel ($Ca_V2.1$), encoded by the *cacophony* gene, block both the rapid induction and the sustained expression of synaptic homeostasis. These data identify a presynaptic protein necessary for the homeostatic modulation of synaptic efficacy following postsynaptic neurotransmitter receptor blockade. We present a model for the role of presynaptic calcium channels during the retrograde, homeostatic regulation of transmitter release at the NMJ.

Results

We have conducted a series of experiments of increasing temporal resolution to define the time course of synaptic homeostasis at the *Drosophila* NMJ. We previously demonstrated that muscle-specific expression of the Kir2.1 potassium channel (*UAS-Kir2.1-GFP*) throughout the 4 days of synapse development at the *Drosophila* larval NMJ specifically inhibits muscle excitability and initiates a homeostatic, compensatory increase in quantal content (Paradis et al., 2001). In the first set of experiments, we took advantage of a temperature-sensitive *GAL80* transgene driven by the tubulin promoter (*TubGAL80ts*) (McGuire et al., 2003) to temporally restrict muscle-specific, *GAL4*-dependent expression of *UAS-Kir2.1-GFP* (see Figure S1 in the Supplemental Data available online). Using these reagents we restricted robust, muscle-specific expression of *UAS-Kir2.1-GFP* to the final 24 hr of larval development (Figures S1 and S2). Importantly, we observed a homeostatic increase in quantal content that is quantitatively identical to the homeostatic increase in quantal content observed following 4 days of *UAS-Kir2.1-GFP* muscle expression (Figure S2). There is no change in bouton number (data not shown; Paradis et al., 2001) or active zone density following 24 hr of *UAS-Kir2.1-GFP* muscle expression, suggesting that homeostatic compensation occurs through modulation of existing synaptic machinery (Figures S2D and S2E). Together, these data demonstrate that synaptic homeostasis can be induced at the mature NMJ within an intact, behaving animal.

Rapid Induction of Synaptic Homeostasis following Postsynaptic Receptor Blockade

We next sought to refine the time necessary to induce synaptic homeostasis. It was previously shown that null mutations in a postsynaptic AMPA/kainate-type glutamate receptor subunit (*GluRIIA*) lead to a decrease in spontaneous miniature excitatory postsynaptic potential (mEPSP) amplitude and a compensatory increase in quantal content (Petersen et al., 1997). To refine the time course of this homeostatic compensation, we turned to pharmacological manipulation of postsynaptic glutamate receptor function. We first characterized the properties of philanthotoxin-433 (PhTox), an insect glutamate receptor antagonist originally purified from wasp venom (Eldefrawi et al., 1988; Karst and Piek, 1991). We demonstrate that PhTox is a persistent, use-dependent inhibitor of postsynaptic glutamate receptors at the *Drosophila* NMJ (Figures 1A–1D). PhTox bath application (4 μM) rapidly inhibits both excitatory postsynaptic potential (EPSP) amplitudes and mepsp amplitudes without

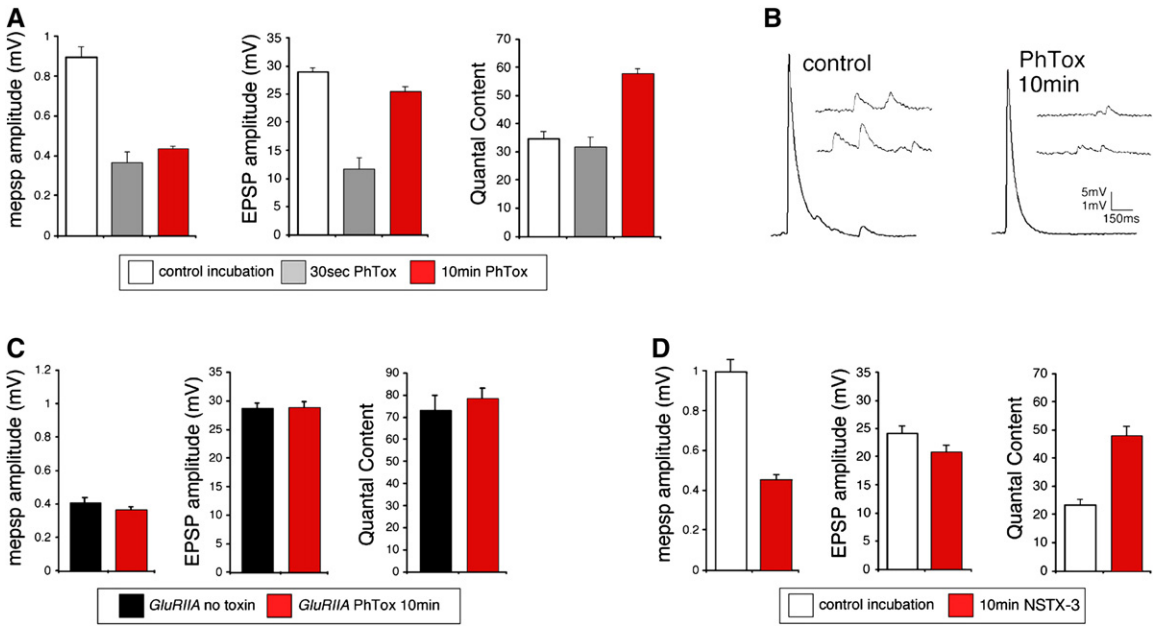

Figure 2. Rapid Induction Synaptic Homeostasis in a Semi-Intact Preparation

(A) Quantification of average mEPSP amplitude (left), average EPSP amplitude (middle), and quantal content (right) for the three conditions listed below the graphs; 10 min saline incubation (control incubation), 30 s incubation in PhTox (30 s PhTox), and a 10 min incubation in PhTox (10 min PhTox). There is a statistically significant increase in quantal content after a 10 min PhTox incubation ($n = 48$; $p < 0.01$) compared to a 30 s PhTox incubation ($n = 10$) or saline incubation (control incubation; $n = 42$).

(B) Sample traces prior to and following PhTox incubation for 10 min. Scale bar, 150 ms; 5 mV for EPSPs and 150 ms; 1 mV for mEPSPs.

(C) Quantification as in (A). Incubating *GluRIIA* mutants for 10 min in PhTox ($n = 12$) does not reduce average mEPSP amplitude beyond that observed in *GluRIIA* mutants without toxin ($p > 0.2$; $n = 12$) and does not increase quantal content beyond that observed in *GluRIIA* mutants without toxin ($p > 0.5$).

(D) Data are shown for wild-type synapses incubated in control saline (10 min) versus wild-type synapses incubated in NSTX-3 (NSTX-3; 10 μM, 10 min). Prior to recording, synapses were washed in normal saline without NSTX-3. A persistent inhibition of postsynaptic receptors following the wash is shown by the significant decrease in mEPSP amplitudes compared to mock-treated wild-type controls ($p < 0.01$). After a 15 min incubation in NSTX-3, EPSP amplitudes are near wild-type values ($p > 0.1$), and there is a significant increase in quantal content ($p < 0.01$).

Error bars represent SEM.

an immediate effect on quantal content (estimated by average EPSP/average mEPSP amplitude) (Figures 1A–1D). PhTox washout after a 2 min incubation results in only a partial recovery of EPSP and mEPSP amplitudes, demonstrating a persistent component of PhTox receptor blockade (Figures 1C and 1D). The persistent effects of PhTox cannot be accounted for by glutamate receptor internalization. This possibility was assessed by surface labeling epitope-tagged GluRIIA receptors prior to and following PhTox application (Stephanie Albin and G.W.D, unpublished data).

Using PhTox we were able to narrow the time necessary for the induction of synaptic homeostasis in an intact animal to 30 min. We injected PhTox (200 μM) into third-instar larvae, achieving a sub-blocking final toxin concentration that significantly decreased mEPSP amplitudes (Figure 1E). Following PhTox injection, animals were initially paralyzed (within ~30 s), though the heart muscles continued to beat. Larvae remained paralyzed for ~30 min before recovering the ability to move. By comparison, animals injected with carrier saline moved normally within 1 min of injection. We next measured synaptic function 30 min following PhTox injection. The average mEPSP amplitude was decreased 30 min following PhTox injection, and we observed a homeostatic increase in quantal content that restored EPSP amplitudes toward wild-type values (Figure 1E). These data demonstrate that a homeostatic increase in quantal content can be induced within 30 min at the mature NMJ in an intact animal.

In order to precisely define the time necessary to induce synaptic homeostasis, we developed a semi-intact larval neuromuscular preparation (see Experimental Procedures). Using a semi-intact preparation we demonstrate that a 30 s incubation in PhTox decreased mEPSP amplitudes without a change in quantal content. However, a 10 min incubation in PhTox caused a significant increase in quantal content that restored EPSP amplitudes toward wild-type levels (Figures 2A and 2B). These data demonstrate that synaptic homeostasis can be induced following 10 min of impaired postsynaptic receptor function in a semi-intact preparation.

A number of control experiments were performed to ensure that the observed change in quantal content is consistent with the induction of synaptic homeostasis. First, rapid homeostatic compensation occurs in the continued presence of PhTox, demonstrating that these effects are not a consequence of toxin withdrawal (see Figure 4 below). Second, we demonstrate that two additional pharmacological inhibitors of postsynaptic receptors (10 μM NSTX-3 and 4 μM PhTox-343) are also capable of inducing synaptic homeostasis in 10–15 min (Figure 2D and data not shown). Finally, we performed experiments to control for the possibility that PhTox

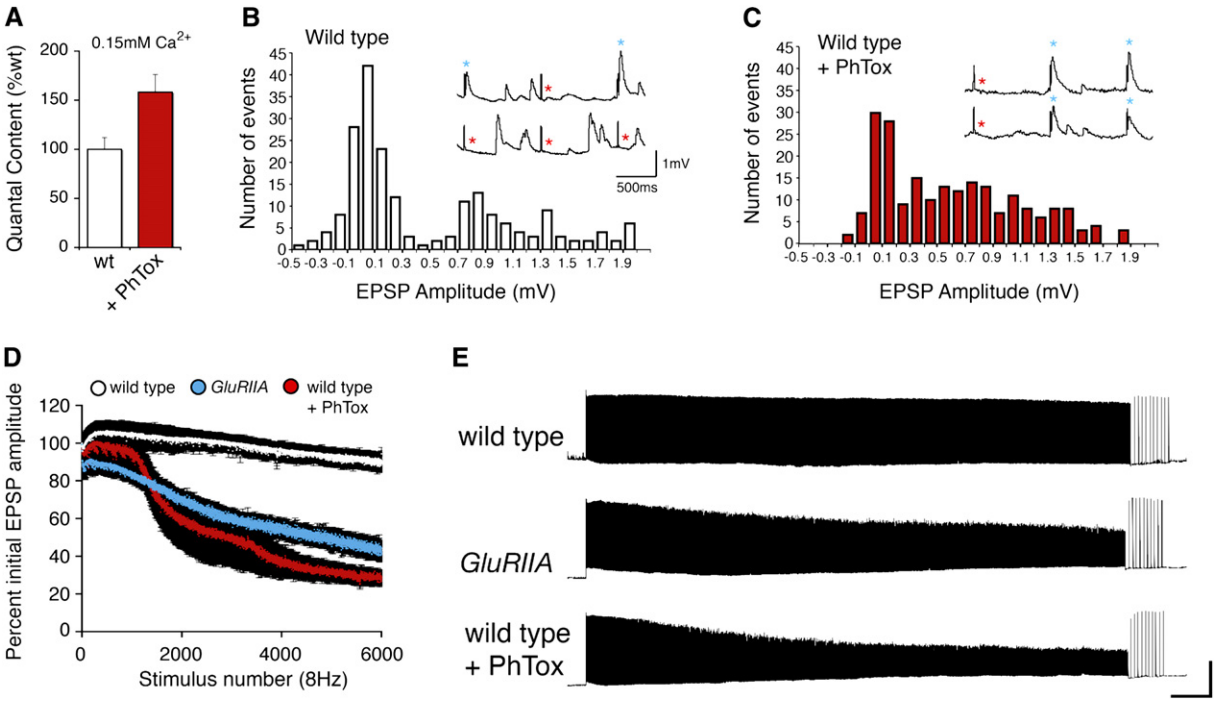

Figure 3. Evidence for Increased Release Probability during the Rapid Induction of Synaptic Homeostasis

(A) Quantal content, estimated by the method of failures, in 0.15 mM Ca^{2+} is significantly increased following application of PhTox (+PhTox; 10 min semi-intact preparation) compared to wild-type in the absence of PhTox ($p < 0.01$). Quantal content values are as follows: wild-type, 0.43 ± 0.04, N = 14; PhTox, 0.68 ± 0.05, N = 15.

(B) Sample histogram of EPSP amplitudes measured in wild-type. Inset shows sample traces from this recording. Three stimuli are shown for each trace (vertical transients are stimulus artifacts). Blue stars indicate stimulus-locked release events, and red stars indicate putative failures following the stimulus artifact.

(C) Sample histogram of EPSP amplitudes measured at a PhTox-treated synapse with inset as in (B).

(D) Graph examining vesicle depletion during a stimulus train (6000 stimuli at 8 Hz) comparing wild-type (white symbols; N = 6) to *GluRIIA* mutant (blue symbols; N = 6) and PhTox-treated (10 min semi-intact; N = 8) animals. The average value (±SEM) is shown for each stimulus to generate the curves. There is significantly greater EPSP rundown comparing GluRIIA and PhTox-treated animals with wild-type ($p < 0.01$).

(E) Sample traces for data shown in (D). There is significantly greater EPSP rundown in *GluRIIA* and PhTox-treated synapses. Rapid recovery to initial EPSP amplitudes is demonstrated by low-frequency stimulation (0.2 Hz) following the cessation of the stimulus train.

Error bars represent SEM.

directly modulates transmitter release by acting upon a presynaptic target. In these experiments, *GluRIIA* null mutant animals were incubated in PhTox for 10 min. *GluRIIA* mutants have decreased quantal size and a homeostatic increase in presynaptic release (Petersen et al., 1997). PhTox treatment did not alter the average mEPSP amplitude compared to mock-treated *GluRIIA* animals, suggesting that PhTox binds with higher affinity to GluRIIA-containing receptor complexes (Figure 2C). Importantly, quantal content remains unaffected compared to mock-treated *GluRIIA* controls, suggesting that PhTox does not directly influence presynaptic release by acting upon an unidentified presynaptic target (Figure 2C). An alternate interpretation could be that the synapse is already maximally potentiated in the *GluRIIA* mutant. However, we find that PhTox treatment can induce a compensatory increase in presynaptic release that is significantly beyond that observed, on average, in the *GluRIIA* mutant animals (compare Figures 2C and 6A). From these data we conclude that PhTox acts primarily to inhibit postsynaptic glutamate receptors and thereby induces a homeostatic increase in quantal content at the *Drosophila* NMJ.

Evidence that the Rapid Induction of Synaptic Homeostasis Is Achieved by a Change in Presynaptic Release Probability

It is thought that the homeostatic increase in synaptic efficacy observed in the *GluRIIA* mutant is due to a change in the probability of presynaptic neurotransmitter release (Petersen et al., 1997). Therefore, we examined whether the rapid induction of homeostatic signaling is also due to a change in the probability of presynaptic release. First, we induced synaptic homeostasis with a 10 min PhTox incubation in a semi-intact preparation and calculated quantal content using the method of failures (0.15 mM Ca^{2+}, 10 mM Mg^{2+} saline). We find a significant 55% increase in quantal content at PhTox-incubated synapses compared to mock-incubated synapses (Figures 3A–3C; $p < 0.001$). These data are consistent with a homeostatic increase in presynaptic release probability following a 10 min incubation in PhTox.

An increase in presynaptic release probability should also result in faster depletion of the vesicle pool during prolonged nerve stimulation. We examined vesicle depletion during prolonged nerve stimulation under conditions of high vesicular release (6000 stimuli at 8 Hz, 2 mM

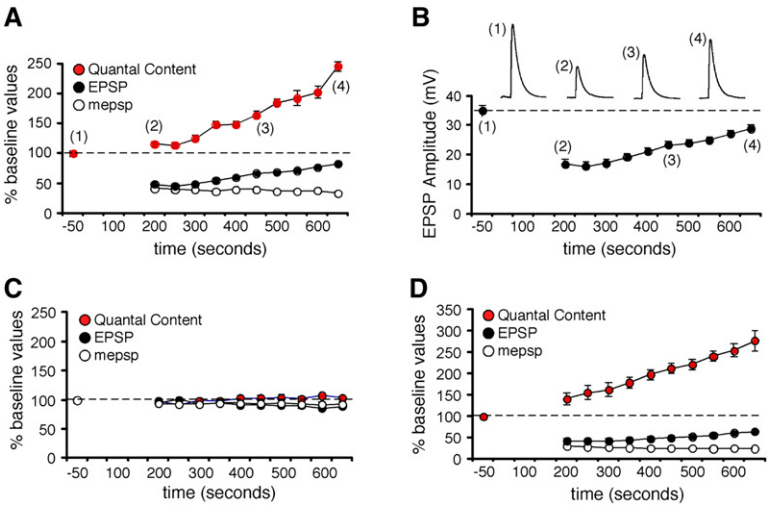

Figure 4. Induction of Synaptic Homeostasis in Real Time

(A) mEPSP, EPSP, and quantal content are plotted over time for a single recording (normalized to baseline values prior to toxin application). Time zero is the time of toxin application. EPSPs delivered at 0.2 Hz are averaged every 50 s. mEPSPs are averaged over identical 50 s intervals. Quantal content is calculated based on these average measurements for each 50 s interval. Baseline stimulation is followed by a perfusion with PhTox (4 μM) that remains present in the bath solution throughout the remainder of the recording. Ten stimuli are delivered immediately following PhTox application to maximally suppress mEPSP amplitudes (amplitudes not shown on graph). 0.2 Hz stimulation is then resumed for the duration of the experiment in the continued presence of PhTox.

(B) EPSP amplitudes for the experiment in (A).

(C) Average values for experiments performed as in (A) without the addition of PhTox (n = 10).

(D) Average values for all experiments that included PhTox as in (A) (n = 12).

Error bars represent SEM.

extracellular Ca^{2+}). We compared wild-type synapses with PhTox-treated synapses (10 min PhTox incubation) and *GluRIIA* mutant synapses (Figures 3D and 3E). Wild-type synapses sustain synaptic transmission without significant depression under these conditions. By contrast, synapses treated with PhTox and *GluRIIA* mutant synapses both show a gradual decline in EPSP amplitudes resulting in significant synaptic depression compared to wild-type ($p < 0.001$). Together with the failure analysis, these data are consistent with a rapid, homeostatic increase in the probability of release following PhTox application. It should be noted that there is not an increase in spontaneous miniature release frequency that parallels the increase in quantal content following PhTox application (data not shown). However, there is also no change in mEPSP frequency in *GluRIIA* mutants that express a homeostatic increase in presynaptic release (Petersen et al., 1997). It is possible that a change in mini frequency is not indicative of altered presynaptic release probability at this synapse or that a population of mEPSP events remains below detection levels in our recordings (Petersen et al., 1997).

Rapid Homeostatic Signaling Is Achieved by a Low-Gain Homeostatic Signaling System

We next sought to characterize the rate of homeostasis at the NMJ in order to address two questions. First, does homeostatic signaling potentiate synaptic efficacy following a delay after toxin application, or is homeostatic signaling initiated immediately? A delay would be indicative of the time over which muscle depolarization is monitored prior to the homeostatic modulation of synaptic efficacy. Second, does the homeostatic increase in synaptic efficacy asymptotically retarget baseline values, implying a low-gain homeostatic system, or is compensation rapid and prone to overshoot baseline values, implying a high-gain homeostatic system (Stelling et al., 2004)? To characterize these properties of synaptic homeostasis we used chronic recordings to follow the induction of homeostatic compensation at single synapses in real time. Initially, following PhTox application (4 μM), both mEPSP and EPSP amplitudes decrease in parallel, and no immediate change in quantal content is observed (Figure 4A). A sample recording made in the continued presence of PhTox shows that mEPSP amplitudes remain at a constant depressed amplitude while EPSP amplitudes gradually increase in size, eventually approaching baseline values (Figures 4A and 4B). Increased EPSP amplitude is associated with a gradual, homeostatic potentiation of quantal content in the continued presence of PhTox (Figure 4A). In some recordings, mEPSP amplitudes continued to decline over the course of the recording while EPSP amplitudes and input resistance remained constant. Again, a gradual increase in quantal content was calculated. When we average our data across all experiments we reveal a gradual monotonic increase in quantal content following a delay of 3–4 min after PhTox application (Figure 4D). Control recordings in the absence of PhTox reveal no change in mEPSP amplitude, EPSP amplitude, or quantal content over the same time interval (Figure 4C). The gradual increase in release is consistent with a low-gain homeostatic system that requires only a short period (2–5 min) during which muscle depolarization is integrated. Finally, consistent with this rapid time course, we present evidence that new protein synthesis is not required for the induction of synaptic homeostasis at the NMJ (Figure S3).

Motoneuron Activity and Evoked Muscle Depolarization Are Not Necessary for the Induction of Synaptic Homeostasis

To test the role of neural activity during the induction of synaptic homeostasis we severed the motor axons on one side of the CNS prior to the application of PhTox to a semi-intact preparation. Axons that remained intact

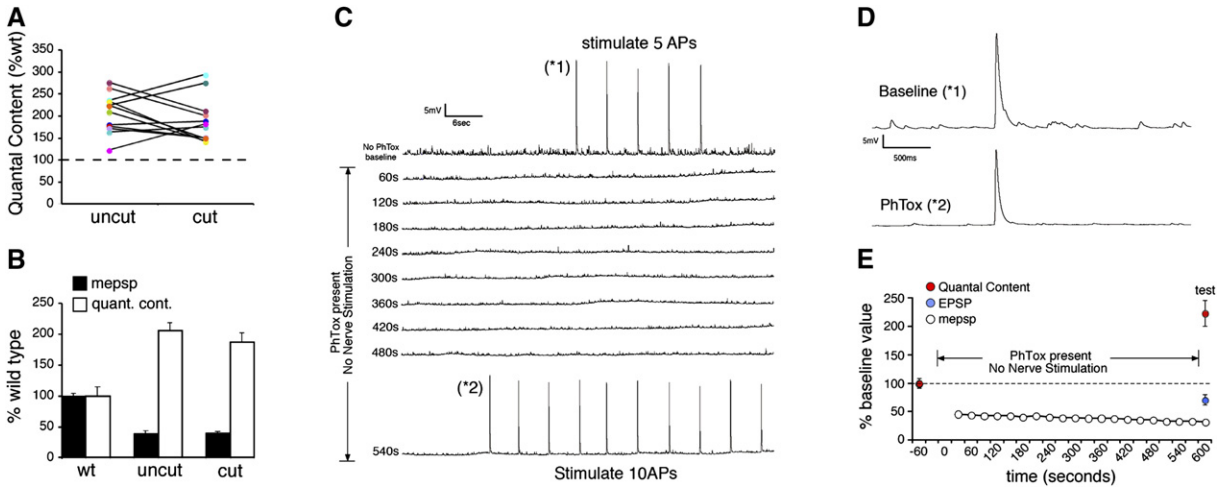

Figure 5. Motoneuron Activity Is Not Required for the Rapid Induction of Synaptic Homeostasis

(A) Quantal content is shown for individual recordings and presented as a percent relative to the average quantal content observed in wild-type animals recorded in normal saline (dotted line at 100%). In each preparation, recordings were made from muscle 6 in segment A3 on both sides of the animal (coded with the same color symbol and connected by a line). In one hemisegment, the motor axons were severed prior to application of PhTox (cut), and in the other hemisegment the motor axons remained intact (uncut). Every recording showed a homeostatic increase in quantal content. There is no obvious trend in the degree of compensation comparing cut versus uncut axons in a single animal.

(B) Average values for the data presented in (A). The cut axons show a statistically significant increase in quantal content compared to controls ($p < 0.01$). The quantal content recorded in uncut axons is not significantly greater than that observed in cut axons ($p > 0.1$).

(C) A sample 10 min recording showing the induction of synaptic homeostasis in the absence of evoked transmission. The recording is initiated in the absence of PhTox, and five stimuli are delivered to quantify basal synaptic efficacy (*1). PhTox is then applied without further nerve stimulation. The absence of evoked neurotransmission is evident until test stimuli are delivered at the end of the recording (ten action potentials; *2).

(D) Sample EPSPs from the recording in (C) from the indicated time points. At time point (*2), the EPSP amplitude is close to baseline, while mEPSPs are significantly smaller than baseline.

(E) Average data for experiments as in (C) calculating quantal content (red), EPSP amplitude (blue), and mEPSP amplitude (white). The average mEPSP amplitude is calculated at 30 s intervals. No evoked release was observed during PhTox incubation until test stimuli are delivered at the end of the recording. In the absence of evoked neurotransmission, PhTox application (over time indicated) induces a significant, homeostatic increase in quantal content compared to baseline values prior to PhTox application ($p < 0.01$).

Error bars represent SEM.

on the other side of the CNS served as an internal control. *Drosophila* motor axons rarely, if ever, fire spontaneous action potentials when the segmental nerve is cut (G.W.D., unpublished data). Consistently, muscle contraction was not observed on the half of the animal where the motor axons were severed, and spontaneous action potentials were never observed during chronic recordings in the presence of a severed motor axon (see below).

We examined the PhTox-dependent induction of synaptic homeostasis by comparing recordings from muscles with cut motor axons on one side of the animal to recordings from muscles in the same abdominal segment on the other side of the animal innervated by intact motor axons (Figures 5A and 5B). We find that homeostatic compensation is always present at synapses with a cut motor axon, indicating that motoneuron action potentials and evoked neurotransmitter release are not required for the induction of synaptic homeostasis (Figures 5A and 5B). As a control, we have recorded, chronically, from NMJs innervated by cut motor axons for 10–15 min and demonstrate that cutting the motor axon alone is not sufficient to potentiate neurotransmitter release at the NMJ (Figure 4C). In addition, we have recorded from semi-intact preparations in which the nerve was cut, and the preparations experience no activity or nerve stimulation for 10–15 min. There was no change in quantal content comparing animals with a cut nerve (quantal content = 33.3 ± 4.0) to wild-type controls recorded immediately following dissection (quantal content = 35.3 ± 1.6; $p > 0.5$). Thus, the absence of action potentials in the motor nerve does not induce a change in presynaptic release. Finally, we have performed chronic recordings to follow the induction of synaptic homeostasis in the absence of nerve stimulation and thereby document the absence of evoked neurotransmission during the induction of synaptic homeostasis. Prior to PhTox application, the nerve was stimulated briefly to quantify baseline presynaptic release. PhTox was then added, and the recording was continued in the absence of stimulation for 9 min before we again tested evoked synaptic transmission (Figures 5C–5E). The muscle recordings document a complete absence of evoked synaptic transmission (Figure 5C). We observe a significant, homeostatic increase in presynaptic release in the absence of neural activity (Figures 5D and 5E) that is quantitatively similar to chronic recordings where nerve stimulation was present (Figure 4D). Taken together, these data suggest that the altered efficacy of spontaneous miniature release events that persist in the absence of evoked neurotransmission can initiate a homeostatic change in presynaptic release.

If synaptic homeostasis does not require evoked neurotransmission, then synaptic homeostasis should also be independent of the muscle safety factor. Neuromuscular synapses, including those in *Drosophila*, release 50%–100% more neurotransmitter than is necessary to

depolarize the muscle to contract (Marrus and DiAntonio, 2005). This excess release is classically referred to as a "safety factor." If impaired muscle contraction initiates homeostatic signaling at the NMJ, then a homeostatic change in presynaptic release should not be induced until muscle excitation (assessed by mEPSP amplitude) falls below some threshold value related to the safety factor, and, at that point, we should observe a significant increase in presynaptic release. We plotted average mEPSP amplitudes versus quantal content for individual recordings from wild-type NMJs with or without PhTox treatment. There is no evidence for a threshold induction of synaptic homeostasis. Instead, quantal content scales precisely with the change in mEPSP amplitude (Figure 6A). A similar relationship is observed when we examine recordings from *GluRIIA* null mutant and wild-type animals on a similar plot (Figure 6B). Although PhTox-treated preparations appear to demonstrate perfect compensation, it should be noted that our recordings were made in the absence of PhTox, which should increase the measured mEPSP amplitudes by ~25% (Figure 1C). Taking this into account the GluRIIA and PhTox-treated preparations should appear similar, falling just to the left of the line indicating perfect homeostatic compensation (Figures 6A and 6B). Two conclusions can be made from these data. First, these data argue that synaptic homeostasis at the NMJ is independent of the muscle safety factor and support the observation that evoked muscle depolarization is not required for the rapid induction of synaptic homeostasis in PhTox-treated animals and, perhaps, the *GluRIIA* mutants as well. Second, these data demonstrate that homeostatic modulation of presynaptic transmitter release is precisely controlled by the homeostatic signaling system such that it is able to precisely offset even small changes in postsynaptic quantal size.

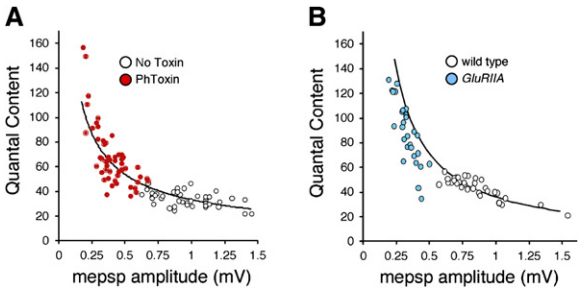

Figure 6. Presynaptic Release Precisely Offsets Decreased Quantal Size

Data for individual recordings are shown, plotting quantal content versus mEPSP amplitude. Each point is a separate experiment. (A) Wild-type synapse (white) and synapses incubated in PhTox for 10 min (red) are shown. Quantal content scales continuously with decreased mEPSP amplitude. The line represents the function describing perfect compensation (quantal content/mEPSP = constant EPSP). The constant EPSP value is taken as the average wild-type amplitude (no drug). (B) Data plotted as in (A) for wild-type (white) versus *GluRIIA* mutant animals.

Synaptic Homeostasis Is Disrupted by Mutations that Disrupt the Pore-Forming Subunit of $Ca_V2.1$ Encoded by *cacophony*

To identify the molecular mechanisms responsible for synaptic homeostasis we initiated a candidate screen for mutations that prevent the rapid induction of synaptic homeostasis at the *Drosophila* NMJ. Altered calcium channel function could, in principle, mediate a rapid homeostatic modulation of presynaptic release probability. Therefore, we genetically tested the involvement of presynaptic calcium channels in the mechanisms of synaptic homeostasis. In *Drosophila*, the *cacophony* (*cac*) gene encodes the α-1 subunit of the $Ca_V2.1$ channel. This channel is exclusively expressed in the nervous system (Tomancak et al., 2002; see also Berkeley *Drosophila* Genome Project); the protein is restricted to the presynaptic terminal, localizes to the presynaptic active zone, and is absolutely required for stimulus-evoked neurotransmitter release at the NMJ (Brooks et al., 2003; Smith et al., 1996). In our experiments we took advantage of hypomorphic mutations in the *cac* gene that impair, but do not eliminate, calcium channel function (Brooks et al., 2003; Dellinger et al., 2000; Kawasaki et al., 2000). The cac^{TS2} and cac^{S} mutations are hypomorphic alleles that, when raised at room temperature, cause a deficit in basal synaptic transmission when recordings are made in 0.5 mM extracellular calcium (cac^{TS2} = 47% decrease in EPSP amplitude; cac^{S} = 71% decrease in EPSP amplitude; absolute amplitudes are presented in Table 1) (Dellinger et al., 2000; Kawasaki et al., 2000). The cac^{TS2} mutation is a missense mutation (P1385S) in the cytoplasmic C-terminal domain of the channel adjacent to a putative EF-hand motif and near a putative IQ domain (Brooks et al., 2003; Kawasaki et al., 2002). The intragenic suppressor of cac^{TS2}, [*su(TS2)2*], is a missense mutation (F916L) in the S5 transmembrane domain in repeat three (see summary in Brooks et al., 2003). The residues that are altered in both mutations are conserved in mouse and worm. The cac^{S} mutation is a missense mutation (F1029I) in the S6 transmembrane domain in repeat three (Smith et al., 1998).

For the analysis of the *cacophony* mutations, we present data both as raw amplitudes (Table 1) and as normalized to the control genotype (Figures 7–9). In the figures, data are normalized to the appropriate *cacophony* mutant background. This helps to account for changes in baseline neurotransmission and highlight the effects of the *GluRIIA* mutant within a given *cac* mutant background. For example, if we observe that decreased mEPSP amplitude, caused by the presence of the *GluRIIA* mutation, correlates with increased quantal content compared to the appropriate genetic control, then we conclude that homeostatic compensation has occurred, even if absolute synaptic strength remains below that observed in wild-type.

We first demonstrate that PhTox application to the cac^{TS2} mutant decreases mEPSP amplitudes without causing a significant homeostatic increase in presynaptic quantal content, indicating strong suppression of synaptic homeostasis (Figure 7A). As a control, we took advantage of an intragenic suppressor mutation isolated within the cac^{TS2} mutant gene, $cac^{TS2}cac^{su(TS2)2}$ (Brooks et al., 2003). Channel function is significantly restored in the $cac^{TS2}cac^{su(TS2)2}$ double mutant, as demonstrated by the restoration of EPSP amplitudes toward wild-type values (Table 1; wild-type EPSP = 33.9 ± 0.7 mV and $cac^{TS2}cac^{su(TS2)2}$ = 26.5 ± 2.0 mV—recorded

Table 1. Physiological Data Demonstrating a Role for *cacophony* in Synaptic Homeostasis

Condition	Figure	Genotype	mEPSP	EPSP	Quantal Content	N
0.5 mM Ca^{2+}	8A, 9A	wt	0.85 (0.03)	33.9 (0.7)	41.8 (1.5)	33
Reared at 22ºC	8A, 9A	*GluRIIA*	0.32 (0.01)	24.1 (0.9)	77.0 (4.0)**	31
	8B	cac^S/+	0.75 (0.03)	29.2 (1.7)	39.5 (1.8)	21
	8B	cac^S/+; *GluRIIA*	0.32 (0.02)	17.0 (0.8)	55.5 (4.2)** (**a**)	16
	8C	cac^S	0.82 (0.07)	10.3 (2.0)	13.9 (3.0)	9
	8C	cac^S; *GluRIIA*	0.39 (0.02)	7.2 (1.1)	18.2 (2.6) ns ^	8
1.5 mM Ca^{2+}	8D, 9D	wt	0.62 (0.04)	36.7 (2.2)	118.3 (10.2)	17
Reared at 22ºC	8D, 9D	*GluRIIA*	0.40 (0.03)	40.8 (2.1)	212.9 (25.6)**	7
	8E	cac^S	0.67 (0.06)	32.5 (2.1)	85.5 (8.4)	7
	8E	cac^S; *GluRIIA*	0.39 (0.02)	20.7 (1.3)	73.8 (4.4) ns ^	6
0.5 mM Ca^{2+}	9A	cac^{TS2}	0.93 (0.04)	18.1 (2.1)	19.6 (2.3)	11
Reared at 22ºC	9A	cac^{TS2}; *GluRIIA*	0.35 (0.01)	13.3 (2.0)	38.3 (8.5)**	13
0.5 mM Ca^{2+}	9B	wt	0.68 (0.03)	28.7 (2.6)	42.7 (2.0)	7
Reared at 29ºC	9B	*GluRIIA*	0.34 (0.03)	27.6 (2.9)	80.1 (5.3)**	6
	9B	cac^{TS2}	0.66 (0.02)	14.0 (1.5)	22.2 (1.9)	11
	9B	cac^{TS2}; *GluRIIA*	0.35 (0.01)	9.8 (1.4)	27.7 (3.5) ns ^	13
	9C	cac^{TS2},$cac^{su(TS2)2}$	0.78 (0.07)	29.1 (3.6)	37.5 (3.4)	8
	9C	cac^{TS2},$cac^{su(TS2)2}$; *GluRIIA*	0.27 (0.01)	14.7 (0.8)	55.1 (4.7)** (**b**)	6
1.5 mM Ca^{2+}	9D	cac^{TS2}	0.71 (0.07)	36.8 (1.9)	100.1 (10.6)	6
Reared at 29ºC	9D	cac^{TS2}; *GluRIIA*	0.37 (0.02)	27.6 (3.7)	125.2 (27.7) ns ^	6
0.5 mM Ca^{2+}	9E	cac^{TS2}	1.07 (0.07)	26.6 (1.4)	25.7 (2.1)	10
29ºC for 24hr	9E	cac^{TS2}; *GluRIIA*	0.40 (0.02)	13.2 (1.3)	33.0 (3.1)*	11

Gray shading identifies recordings made under identical conditions. Boxes group data sets presented within single graphs in Figures 8 and 9 and compared statistically. Note: The column titled "Figure" indicates the location of these data within Figures 8 and 9. Data recorded at 1.5 mM extracellular calcium are corrected for nonlinear summation. * indicates significance at p = 0.03 compared to cac^{TS2} reared under identical conditions. ** indicates significance at $p \leq 0.01$ compared to the genotype within the same box. "ns" indicates p > 0.25 compared to the genotype within the same box. (a) Quantal content in cac^S/+;*GluRIIA* is significantly less than *GluRIIA* alone shown in Figure 8A, p < 0.01. (b) Quantal content in cac^{TS2},$cac^{su(TS2)2}$;*GluRIIA* is significantly smaller than *GluRIIA* in Figure 9B, p < 0.01, and significantly greater than wild type in Figure 9B, p < 0.05. ^ indicates that quantal content is different than *GluRIIA* alone under identical conditions (p < 0.01). EPSP and mEPSP are in mV(SEM).

at room temperature) (Brooks et al., 2003). When PhTox is applied to the $cac^{TS2}cac^{su(TS2)2}$ animals, acute synaptic homeostasis is significantly restored (Figure 7B). It should be noted that synaptic homeostasis does not reach the levels observed in wild-type animals. This is consistent with the observation that the intragenic

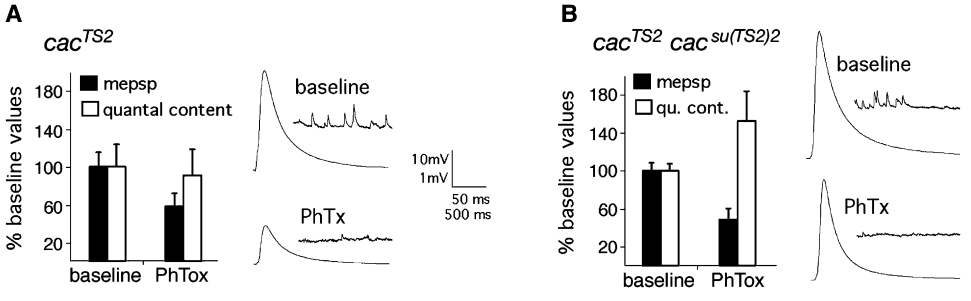

Figure 7. The Induction of Synaptic Homeostasis Is Suppressed by Mutations in the $Ca_V2.1$ α-1 Subunit

(A) Average mEPSP and quantal content, normalized to baseline, for cac^{TS2} animals with and without PhTox incubation (10 min). Sample traces are at right. No homeostatic increase in quantal content is observed following PhTox incubation (p > 0.4; n = 13).

(B) Quantification as in (A) for the $cac^{TS2}cac^{su(TS2)2}$ intragenic suppressor double mutation. Sample traces at right, scale as in (A). A homeostatic increase in quantal content is restored in the $cac^{TS2}cac^{su(TS2)2}$ double mutant (p < 0.02; n = 13).

Error bars represent SEM.

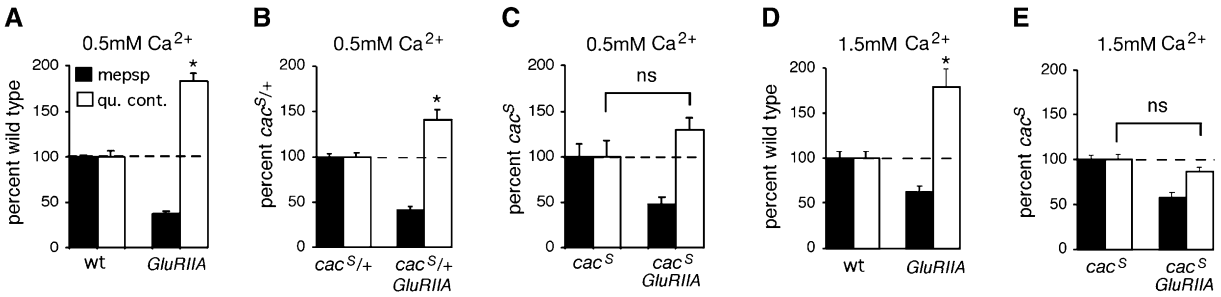

Figure 8. The Expression of Synaptic Homeostasis Is Suppressed by Mutations in the $Ca_V2.1$ α-1 Subunit

(A) Quantification of average mEPSP amplitude (filled bars) and quantal content (open bars). Values are normalized to wild-type control (dotted line). *GluRIIA* mutants have decreased mEPSP amplitudes and a homeostatic increase in quantal content ($p < 0.001$ for both).

(B) Values as in (A) are normalized to those observed in the *cac*^{S}/+ heterozygous condition. A homeostatic increase in quantal content is observed in the *cac*^{S}/+;*GluRIIA* animals ($p < 0.01$). However, the magnitude of the increase in quantal content is significantly less than that observed in *GluRIIA* mutants shown in (A) ($p < 0.01$).

(C) Quantification as in (A) for control and *cac*^{S};*GluRIIA* double mutants. Data are normalized to values observed in *cac*^{S} alone. A homeostatic increase in quantal content is suppressed in the *cac*^{S};*GluRIIA* double mutant compared to *cac*^{S} alone ($p > 0.2$).

(D) Quantification as in (A) for control and *GluRIIA* mutants recorded in 1.5 mM extracellular calcium. *GluRIIA* mutants show a compensatory increase in quantal content at 1.5 mM extracellular calcium compared to wild-type ($p < 0.01$). Quantal contents were corrected for nonlinear summation prior to normalization.

(E) The homeostatic increase in quantal content is suppressed in the *cac*^{S};*GluRIIA* double mutant compared to *cac*^{S} mutants alone, recorded in 1.5 mM extracellular calcium ($p > 0.5$).

Error bars represent SEM.

suppressor mutation improves channel function, but does not recapitulate a wild-type channel (Brooks et al., 2003). It remains unknown how the intragenic suppressor mutation alters channel function. However, at a minimum, these data support the conclusion that a mutation in *cacophony* is the cause of altered homeostasis in the *cac*^{TS2} animal and that presynaptic Cacophony (α subunit of presynaptic $Ca_V2.1$) is required for the rapid, homeostatic modulation of transmitter release.

We next tested whether *cac* mutations block synaptic homeostasis when placed in the *GluRIIA* mutant background. These experiments test whether the induction of synaptic homeostasis is achieved by similar mechanisms in *GluRIIA* mutants and PhTox-treated animals and test whether the expression of synaptic homeostasis over 4 days of development also requires Cacophony. We generated double mutant animals, combining a null allele of *GluRIIA* with either *cac*^{S} or *cac*^{TS2} and generated a triple mutant by combining *GluRIIA* with *cac*^{TS2}*cac*$^{su(TS2)2}$. First, we demonstrate that synaptic homeostasis is suppressed in the *cac*^{S};*GluRIIA* double mutant animals (compare Figures 8A and 8C). These data indicate that synaptic homeostasis in the *GluRIIA* mutants also requires normal presynaptic Cacophony function.

Since baseline neurotransmission is compromised in the *cac*^{S} mutant, it remains possible that decreased calcium influx through the mutant *cac*^{S} channel cannot support increased vesicle release of any kind. To address this issue we performed two control experiments. First, we asked whether heterozygous (*cac*^{S}/+) mutants suppress synaptic homeostasis in the *GluRIIA* mutant background. The baseline EPSP amplitudes in *cac*^{S}/+ animals are nearly wild-type, indicating that these synapses can support near-normal transmitter release (wild-type EPSP = 33.9 ± 0.7 mV and *cac*^{S}/+ = 29.2 ± 1.7 mV, $p < 0.01$). A significant increase in quantal content is observed in the *cac*^{S}/+;*GluRIIA* double mutant compared to *cac*^{S}/+ alone, indicating significant homeostatic compensation (Figure 8B). However, the magnitude of this homeostatic compensation is less than that observed in *GluRIIA* mutants alone, indicating that the *cac*^{S}/+ heterozygous condition suppresses homeostatic compensation without substantially altering baseline neurotransmission (compare Figures 8A and 8B; $p < 0.01$). As a further control, we asked whether the expression of synaptic homeostasis could be restored in the *cac*^{S};*GluRIIA* double mutant animals by recording in elevated extracellular calcium. At 1.5 mM extracellular Ca^{2+}, EPSP amplitudes are restored to wild-type levels in the *cac*^{S} animals (wild-type EPSP amplitude = 36.7 ± 2.2 mV while *cac*^{S} = 32.5 ± 2.1 mV; $p > 0.3$, Table 1). However, synaptic homeostasis remains blocked in the *cac*^{S};*GluRIIA* double mutants (Figures 8D and 8E). Since 1.5 mM extracellular calcium supports near-normal vesicular release in the *cac*^{S} background, limited calcium influx is unlikely to simply mask the expression of synaptic homeostasis in the *cac*^{S};*GluRIIA* double mutants.

Finally, to confirm that Cacophony functions presynaptically during synaptic homeostasis (as predicted by expression analysis) we rescued a *cacophony* null mutation by presynaptic expression of a *UAS-cacophony-GFP* transgene (Kawasaki et al., 2002, 2004) and did so in the presence of the *GluRIIA* mutation. We observe a robust, homeostatic increase in quantal content in these rescued animals ($p < 0.01$ compared to wild-type) that is similar to that seen in *GluRIIA* mutants alone ($p = 0.15$ compared to *GluRIIA*), demonstrating that presynaptic Cacophony is sufficient to mediate synaptic homeostasis (values for *elaV-GAL4, cac*^{null}/Y; *UAS-cac-GFP*, *GluRIIA*/*GluRIIA* recordings: quantal content = 66.4 ± 5.7, EPSP amplitude = 27.4 mV ± 2.5, quantal size = 0.41 mV ± 0.02). Since presynaptic Cacophony supports normal homeostatic compensation, these data provide important molecular confirmation that a retrograde signal mediates synaptic homeostasis at this synapse.

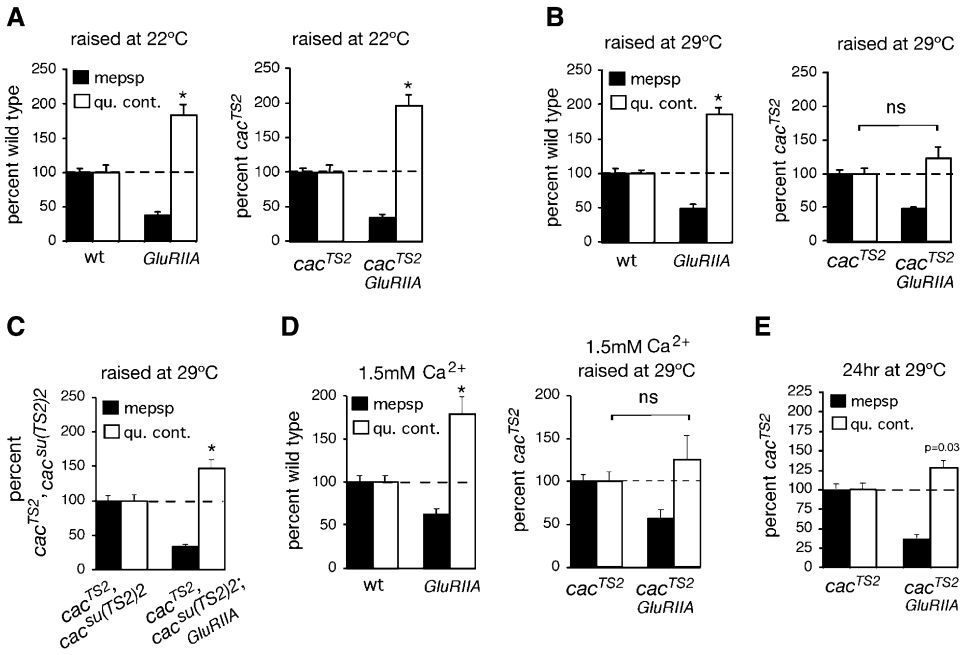

Figure 9. Conditional Disruption of Synaptic Homeostasis using Temperature-Sensitive Mutations in the $Ca_V2.1$ α-1 Subunit

(A) Quantification of average mEPSP amplitude (filled bars) and quantal content (open bars). Values are normalized to wild-type control (dotted line) recorded in 0.5 mM extracellular calcium. (Left) *GluRIIA* mutants have decreased mEPSP amplitudes and a homeostatic increase in quantal content ($p < 0.001$ for both). Data are replotted from Figure 8A for figure clarity. (Right) There remains a significant homeostatic increase in quantal content in the *cac^{TS2};GluRIIA* double mutant compared to *cac^{TS2}* alone ($p < 0.01$).

(B) Quantification as in (A) for wild-type (wt), *GluRIIA*, *cac^{TS2}*, and *cac^{TS2};GluRIIA* raised at 29°C (assayed at room temperature, 0.5 mM Ca^{2+}). (Left) *GluRIIA* animals show a compensatory increase in quantal content compared to wild-type ($p < 0.01$). At right, the *cac^{TS2};GluRIIA* double mutants fail to show a homeostatic increase in quantal content when compared to *cac^{TS2}* alone ($p > 0.25$).

(C) Quantification as in (A) for the double mutant *cac^{TS2},cac$^{su(TS2)2}$* and the triple mutant *cac^{TS2},cac$^{su(TS2)2}$;GluRIIA* raised at 29°C (assayed at room temperature, 0.5mM Ca^{2+}). Values are normalized to *cac^{TS2},cac$^{su(TS2)2}$*. A homeostatic increase in quantal content is observed in triple mutant animals ($p < 0.01$), indicating partial restoration of homeostatic compensation by the intragenic suppressor mutation.

(D) Quantification as in (A) for wild-type (wt), *GluRIIA*, *cac^{TS2}*, and *cac^{TS2};GluRIIA* for the indicated calcium and rearing conditions. Data for wt and *GluRIIA* are repeated from Figure 8D for visual clarity. At right, the *cac^{TS2};GluRIIA* double mutants fail to show a significant increase in quantal content compared to *cac^{TS2}* alone ($p > 0.25$). Quantal contents were corrected for nonlinear summation prior to normalization.

(E) *cac^{TS2}* and *cac^{TS2};GluRIIA* animals were raised at room temperature for 3 days of larval development before being shifted to 29°C for the final 24 hr of larval development. A homeostatic increase in quantal content is observed ($p = 0.03$). However, the homeostatic increase in quantal content is significantly suppressed ($p < 0.01$) in the *cac^{TS2};GluRIIA* double mutant animals compared to that observed when *cac^{TS2};GluRIIA* animals are raised at 22°C throughout development (A—right graph). Furthermore, the increase in quantal content is not different from that observed when *cac^{TS2};GluRIIA* animals are raised at 29°C throughout development (B—right graph). Throughout, the notation "ns" indicates that quantal content is not significantly different ($p > 0.25$). Sample size for each genotype and non-normalized values (including EPSP amplitudes) are presented in Table 1.

Error bars represent SEM.

A consistent but more complex set of data were obtained for the *cac^{TS2};GluRIIA* double mutants. When the *cac^{TS2};GluRIIA* double mutants are raised at room temperature (22°C) there is no deficit in synaptic homeostasis (Figure 9A). This is in contrast to the observation that the *cac^{TS2}* mutation, when raised at room temperature, blocks PhTox-induced synaptic homeostasis (Figure 7). This discrepancy could be explained if the *cac^{TS2}* mutations delay the induction of synaptic homeostasis without fully blocking the process. This is consistent with observations in other homeostatic signaling systems where mutations can slow the process of homeostatic compensation without blocking the mechanism (Davis, 2006). Thus, normal synaptic homeostasis could be achieved over the 4 days of larval development in the *cac^{TS2};GluRIIA* double mutants. To test this idea, we raised *cac^{TS2};GluRIIA* double mutants at an intermediate, nonpermissive temperature (29°C), thereby making the *cac^{TS2}* mutation more severe during development. Baseline quantal content, assayed at room temperature, is unchanged by raising *cac^{TS2}* at 29°C compared to *cac^{TS2}* raised at room temperature (Table 1). This indicates that functional synapse development has not been impaired by rearing *cac^{TS2}* animals at 29°C. However, synaptic homeostasis is now fully suppressed in the *cac^{TS2};GluRIIA* double mutant (Figure 9B). Again, as a control, we demonstrate that synaptic homeostasis is significantly restored in the *cac^{TS2}cac$^{su(TS2)2}$;GluRIIA* triple mutant animals raised in parallel at 29°C and assayed at room temperature (Figure 9C). Quantal content in the *cac^{TS2}cac$^{su(TS2)2}$;GluRIIA* triple mutant is not only significantly elevated beyond the appropriate genetic control (*cac^{TS2}cac$^{su(TS2)2}$*), but it is increased compared to wild-type animals ($p < 0.05$), supporting the conclusion that some homeostatic signaling has been restored. However, as observed in PhTox experiments, the presence of the intragenic suppressor mutation does not restore synaptic homeostasis to levels observed in the

GluRIIA mutant alone, consistent with $cac^{TS2}cac^{su(TS2)2}$ lacking full functionality. As a further control we assayed synaptic homeostasis at elevated calcium (1.5 mM Ca^{2+}) for the cac^{TS2};*GluRIIA* animals raised at 29°C. As observed for the cac^{S} animals, baseline transmission is restored toward wild-type levels in the cac^{TS2} controls assayed at elevated calcium (wild-type = 36.7 ± 2.2 mV and cac^{TS2} = 36.8 ± 1.9 mV in 1.5 mM Ca^{2+}, Table 1), but synaptic homeostasis remains severely impaired (Figure 9D).

We also controlled for possible developmental abnormalities caused by the *cacophony* mutations. It has been previously reported that mutations in the *cacophony* gene result in decreased synaptic growth (Rieckhof et al., 2003; Xing et al., 2005). However, these prior studies utilized mutations and experimental conditions that are different and possibly more severe than those utilized here. In order to determine whether altered synaptic homeostasis in the *cacophony* mutations is a secondary consequence of impaired synaptic growth we controlled for possible anatomical developmental abnormalities associated with raising cac^{TS2} mutants at 29°C or with the cac^{S} animals raised at room temperature (conditions that block homeostasis). There is no change in synaptic bouton number in animals harboring either the cac^{TS2} or cac^{S} homozygous mutations raised under conditions that block synaptic homeostasis (Figure S4). Thus, impaired synaptic homeostasis in these animals is not a secondary consequence of altered synapse development. Together, these data support the conclusion that presynaptic *cacophony* is necessary for the induction and expression of synaptic homeostasis at the *Drosophila* NMJ.

Cacophony Is Necessary for the Sustained Expression of Synaptic Homeostasis

It remains unknown whether synaptic homeostasis at the NMJ is reversible. Homeostatic quantal scaling in the vertebrate CNS decays over a period of days following the removal of chronic activity manipulations (Thiagarajan et al., 2005). If homeostatic compensation is labile, then it may be necessary for the muscle to continually invoke homeostatic signaling to counteract developmental perturbations such as the *GluRIIA* mutation. Thus, a remaining question is whether the Cacophony channel is also necessary for the sustained expression of homeostatic compensation. We addressed this question by performing a temperature-shift experiment on cac^{TS2};*GluRIIA* double mutant animals. The cac^{TS2};*GluRIIA* double mutants show normal homeostasis when raised at room temperature, but severely impaired homeostasis when raised at 29°C. Therefore, we raised cac^{TS2};*GluRIIA* animals at room temperature and asked whether a shift to 29°C for the final 24 hr of larval development was sufficient to block synaptic homeostasis (Figure 9E). We find that homeostatic compensation is strongly suppressed following a 24 hr shift to 29°C in the third larval instar (Figure 9E). Although a statistically significant increase in quantal content above baseline is observed, the magnitude of this change is not statistically different from the cac^{TS2};*GluRIIA* double mutants that are raised continually at 29°C ($p > 0.4$, compare Figures 9E and 9B). As a control, we demonstrate that synaptic homeostasis is unaltered in *GluRIIA* mutant animals that are raised at 29°C throughout the 4 days of larval development (Figure 9B). These data suggest that the normal functionality of presynaptic Cacophony is necessary for the sustained expression of synaptic homeostasis.

Discussion

Rapid Induction of Homeostatic Signaling at the *Drosophila* NMJ

Here we demonstrate that robust homeostatic modulation of presynaptic release can be observed in as little as 2–3 min and that the full expression of homeostatic compensation can be achieved in 10 min (Figure 4). By comparison, homeostatic compensation at the vertebrate NMJ following pharmacological AChR blockade requires several days to be expressed (Plomp et al., 1992, 1994). Similarly, in the central nervous system, homeostatic modulation of synaptic efficacy requires several hours (Sutton et al., 2006) and often several days before detectable changes are observed (Desai et al., 2002; Thiagarajan et al., 2005; Turrigiano et al., 1998). Although the speed with which synaptic efficacy is modulated at the *Drosophila* NMJ is surprising, prior phenomenological studies using PhTox in other insects agree well with our data (Eldefrawi et al., 1988; Karst and Piek, 1991). Importantly, the time between postsynaptic receptor blockade and the expression of altered presynaptic release should reflect the time over which postsynaptic excitation is integrated by the homeostatic "sensors" in the muscle. Since altered presynaptic release can be detected within 2–3 min (Figure 4), our data suggest that muscle excitation is being integrated over a time frame of seconds to minutes, far more rapidly than previously thought to occur at the *Drosophila* NMJ, or at any other synapse (Davis, 2006).

Spontaneous Miniature Release Events Can Initiate Rapid and Precise Homeostatic Signaling

It has been suspected that synaptic homeostasis is an activity-dependent phenomenon at the NMJ (Petersen et al., 1997; Davis et al., 1998; Davis and Goodman, 1998; Paradis et al., 2001; Davis and Bezprozvanny, 2001). Here we provide evidence that neither activity in the motoneuron nor evoked neurotransmission is required for the induction of synaptic homeostasis (Figures 4 and 5). These data suggest that the muscle is able to detect a change in postsynaptic receptor function through the action of spontaneous miniature release events. Our data do not rule out the possibility that evoked neurotransmission might normally participate in the induction of synaptic homeostasis. However, a change in the efficacy of spontaneous miniature release events is able to convey sufficient information to induce homeostatic compensation. Interestingly, the speed of homeostatic signaling does not appear to be modulated by the presence or absence of motoneuron activity. Regardless of whether the motor axons remain intact or are severed, homeostatic signaling requires at least 2–3 min before it is observable as a change in presynaptic release and requires 10 min to be fully expressed (Figures 2A, 4, and 5).

If spontaneous miniature release events are sufficient to induce homeostatic signaling, two models could be

considered. First, homeostatic signaling could be induced at individual active zones. The rate of spontaneous release at this synapse is approximately four events per second. If one assumes that there are approximately 300 active zones at the NMJ on muscle 6 (Atwood et al., 1993), then, during the 10 min induction of synaptic homeostasis (assuming an equal probability of spontaneous events across all active zones), each active zone should experience approximately eight vesicles. This suggests that remarkably few vesicles could provide the information at each active zone to achieve precise homeostatic compensation. In support of this possibility, data from the vertebrate central nervous system indicate that mEPSPs can act locally to achieve significant effects on synapse stability (McKinney et al., 1999) and synaptic function (Sutton et al., 2006). However, another model is equally plausible at the NMJ. It is not necessary that precise homeostatic compensation be induced at the level of individual active zones. If the muscle can integrate some aspect of mEPSP efficacy across multiple active zones over time then several hundred individual quantal release events could be utilized to provide the information necessary for the induction of synaptic homeostasis.

What signaling mechanisms are sensitive enough to detect changes in the efficacy or signaling capacity of quantal release events? An attractive possibility is that calcium signaling at the postsynaptic density is involved. *Drosophila* glutamate receptors are calcium permeable. Several studies, including work at the *Drosophila* NMJ, have implicated calcium or calcium-sensitive signaling molecules such as CamKII in the mechanisms of synaptic homeostasis (Haghighi et al., 2003; Marder and Prinz, 2002; Thiagarajan et al., 2002; Turrigiano et al., 1994). Given that active zones throughout the nervous system release and respond to one vesicle (or at most a few vesicles) at any given time, it is plausible that postsynaptic calcium signaling has the sensitivity to detect changes in the efficacy of single vesicles. Consistently, there is evidence that spontaneous miniature release events can influence postsynaptic signaling including CamKII activity (Murphy et al., 1994a, 1994b; Sutton et al., 2004, 2006; Sutton and Schuman, 2005). An appealing feature of this model is that the postsynaptic active zone could be an isolated signaling compartment. At the NMJ this would seem to be necessary in order to isolate calcium signaling at the postsynaptic density from the calcium waves that propagate throughout the t-tubule network during muscle contraction. In support of this idea, the postsynaptic density is enveloped by an elaborate membrane network termed the "subsynaptic reticulum" that could function to isolate the postsynaptic density from the calcium transients experienced during muscle contraction.

In this study we also demonstrate that disruption of muscle membrane excitation via muscle-specific expression of the Kir2.1 potassium channel can initiate synaptic homeostasis within 24 hr at a late stage of synapse development (Figures S1 and S2). These data suggest that a disruption of muscle excitability is sufficient to induce homeostatic compensation (Paradis et al., 2001). It is important to emphasize that these data do not rule out the possibility that altered current flow through GluRs could also be sufficient to induce homeostatic compensation (Paradis et al., 2001). It also remains possible that multiple mechanisms exist to induce homeostatic compensation at the NMJ (Davis, 2006; Davis and Bezprozvanny, 2001). At present, the time necessary for the induction of Kir2.1 expression in muscle prevents us from directly testing whether homeostatic compensation under these conditions requires neural activity.

Homeostatic Control of Presynaptic Release Is Achieved via Presynaptic $Ca_V2.1$ Calcium Channels

Although homeostatic signaling is a robust phenomenon in both the central and peripheral nervous systems, very little is known about the underlying molecular mechanisms (see Davis, 2006, for a recent review). Here we demonstrate that two independent point mutations in the *cacophony* gene block both the rapid induction of synaptic homeostasis in response to application of PhTox and the sustained expression of synaptic homeostasis in glutamate receptor mutants (*GluRIIA*). These data not only identify an important molecular component of homeostatic signaling but also provide important molecular confirmation that synaptic homeostasis is mediated by a retrograde signal from muscle to nerve at this synapse.

In considering the role of the Cacophony channel in synaptic homeostasis, it is important to assess whether the *cacophony* mutations primarily alter synapse development and only secondarily impair homeostatic compensation. At vertebrate central and peripheral synapses, for example, a null mutation in the pore-forming subunit of $Ca_V2.1$ causes diverse developmental defects including altered expression of other calcium channel subunits and changes in synapse morphology and stability (Cao and Tsien, 2005; Piedras-Renteria et al., 2004). Several observations argue against this possibility in our present work. First, because we analyze hypomorphic and temperature-sensitive point mutations, the mutant $Ca_V2.1$ channels remain at the NMJ and should preclude other channels from occupying their preferred position at the active zone (Cao et al., 2004). This idea is supported by the demonstration that temperature-sensitive Cacophony channels can support nearly normal transmitter release at room temperature (1.5 mM Ca^{2+}), but show a pronounced temperature-sensitive defect in neurotransmission at elevated temperature (Brooks et al., 2003). We also do not observe any defect in synaptic growth or synapse morphology in the *cacophony* mutations under the conditions utilized in this study (Figure S4). Although prior work from other laboratories has documented synaptic growth defects associated with *cacophony* mutations, the mutations and conditions used in these prior studies were different and possibly more severe than those used here (Rieckhof et al., 2003; Xing et al., 2005).

Another concern is that the deficit in neurotransmission observed in *cacophony* mutants simply masks our ability to detect an otherwise normal homeostatic change in presynaptic release. However, if this were the case, then the deficit in release that we observe when we record from the synapse should correlate with the degree to which homeostasis is suppressed. Several observations are inconsistent with this expectation. First, the cac^S/+ heterozygous animals have normal

baseline transmission but show a significant impairment in homeostatic compensation. Second, the degree to which the *cac*^{TS2} mutation disrupts homeostasis correlates with the time spent at 29°C but not with a change in baseline transmission assayed at 22°C. These data dissociate the effects of this channel during the induction of homeostasis from its role during basal presynaptic release. Thus, it appears that Cacophony is directly involved in the presynaptic mechanisms that generate a homeostatic change in presynaptic transmitter release.

There are two general mechanisms by which *cacophony* mutations could block homeostatic compensation. The Cacophony channel could be a direct target of the homeostatic, retrograde signal and thereby modulate presynaptic release probability. Alternatively, calcium influx via Cacophony could be a permissive signal for additional signaling within the presynaptic nerve terminal. Such a mechanism would be analogous to the proposed function of presynaptic R-type calcium channels in mossy fiber LTP (Nicoll and Schmitz, 2005). In either case, the involvement of Cacophony in synaptic homeostasis is intriguing given the numerous mechanisms by which the conductance of $Ca_V2.1$ channels can be modulated. For example, both PKC and G protein signaling have been shown to influence $Ca_V2.1$ channel function (Evans and Zamponi, 2006). Thus, any retrograde signal that impinges on these signaling mechanisms could alter the activity of the $Ca_V2.1$ channel and modulate presynaptic release during homeostatic signaling. Recent data indicate that the *cac*^{TS2} mutation alters channel inactivation in heterologous cells, suggesting that modulation of calcium channel inactivation could be involved in the homeostatic modulation of synaptic function (Macleod et al., 2006).

A Revised View of Synaptic Homeostasis at the *Drosophila* NMJ

The data presented here demonstrate that homeostatic signaling can be independent of synaptic growth and development at the NMJ. Rather, homeostatic signaling at the NMJ appears to be a rapid form of plasticity capable of tuning presynaptic transmitter release to offset even small changes in postsynaptic excitability. Furthermore, since synaptic homeostasis can be rapidly induced at a late stage of synapse development, it suggests that the mechanisms of synaptic homeostasis are persistently active at the NMJ. Based upon these new data we propose that synaptic homeostasis represents a mechanism to constrain the variability associated with robust but ultimately imperfect mechanisms of neural development. This property of homeostatic signaling could be particularly important during the development of complex neural circuitry in the CNS because errors that occur early in development could be compounded as additional layers of neural circuitry are established. We further hypothesize that the capacity for homeostatic signaling will be retained throughout the life of an organism to counteract stress-related, disease-related, or injury-related perturbations that alter neural function. In this regard it is interesting to note that mutations in the pore-forming subunit of $Ca_V2.1$ have been linked to migraine and ataxia in humans (Plomp et al., 2001). Altered channel activity and synaptic function have been probed as an underlying cause of these conditions (Barrett et al., 2005; Cao and Tsien, 2005). Together these data suggest a possible link between impaired homeostatic signaling and neurological disease.

Experimental Procedures

Physiology

Recordings were made from muscle 6 in abdominal segment 3 of third-instar larvae as previously described (Davis et al., 1998). Recordings are made in HL3 saline at specified calcium concentrations (see text). Care was taken in all recordings to ensure reliable recruitment of both motoneurons innervating muscle 6 (Davis et al., 1998; Albin and Davis, 2004; Paradis et al., 2001). Semi-intact preparations were achieved by pinning the anterior and posterior extremities of a third-instar larva and then making a dorsal incision. It was essential that the animal not be stretched in the longitudinal or lateral directions since stretching the muscles consistently disrupted the induction of homeostatic compensation (G.W.D., unpublished data). The CNS, fat, and gut were left intact. PhTox (4 μM final concentration) was perfused into the animal through this incision. Robust body wall contractions were initially present, demonstrating continued presence of motoneuron activity. Following a defined period of incubation (see text), the dissection was completed, including the removal of the CNS as previously described (Davis et al., 1998). During chronic recordings, the larvae were dissected without stretching and the CNS removed. The cut motor axon was stimulated as described previously (Davis et al., 1998). In all chronic recordings, muscle input resistance (R_{in}) was monitored at the beginning and end of the recording. Recordings were excluded if R_{in} or V_m changed by more than 20%. In no instance did R_{in} increase during chronic recordings (data not shown). Temperature was controlled during animal rearing in Forma environment chambers with defined temperature and humidity (Forma Scientific). Control animals were reared in parallel and treated identically in all experiments. Philanthatoxin-343, -433, and NSTX-3 (Sigma) were prepared as stock solutions (PhTox, 4 mM in DMSO; NSTX-3, 10 mM in H_2O) and diluted in HL3 saline to the indicated concentration (see text). Larval injections were achieved using glass microelectrodes filled with HL3 saline/PhTox and pressure injection under visual control using an inverted microscope (Zeiss). Following injection, animals were placed at a food source on moist apple juice plates and allowed to recover. In all cases, continued heartbeat was assessed visually with a dissection microscope. Quantal content was calculated for each individual recording by calculating the average EPSP/average mEPSP (Davis et al., 1998; Davis and Goodman, 1998; Paradis et al., 2001; Albin and Davis, 2004). Quantal content was also calculated by the method of failures according to $\ln N/n_0$, where N = trials and n_0 is the number of failures (Petersen et al., 1997; Davis and Goodman, 1998). Quantal contents calculated for each recording were then averaged across animals for a given genotype.

Anatomical Analysis

Third-instar larval fillets were fixed (Bouins) and stained with anti-HRP (DHSB, IA) and either mAb nc82 (gift of Eric Buchner; see Wagh et al., 2006) or anti-GluRIIA [DHSB, IA]). Anti-HRP staining allowed quantification of bouton number as previously described (Albin and Davis, 2004). Active zones visualized by nc82 or anti-GluRIIA were quantified according to previously published methods (Albin and Davis, 2004).

Genetics

Drosophila mutations were utilized as described in the text. *GluRIIA* null mutations are *GluRIIA*^{Sp16} (Petersen et al., 1997). Conditional *Kir2.1-GFP*-expressing animals were generated by crossing *MHC-Gal4, UAS-Kir2.1-GFP/TM6b* females to males carrying the *Tub-Gal80ts* transgene (McGuire et al., 2003; Paradis et al., 2001). One-hour egg lays were performed on apple juice plates. Animals were grown at 18°C through embryogenesis and early larval development. For the "0 Hours of Kir2.1 Expression" condition, animals were raised at 18°C for 8 days. For the "24 Hours of Kir2.1 Expression" condition, animals were raised at 18°C for 7 days and then 30°C for 24 hr. The hypomorphic *cacophony* mutations utilized are *cac*^{S} (Smith et al., 1998), *cac*^{TS2} (Dellinger et al., 2000), and

cac^{TS2}, *cac*$^{su(TS2)2}$ (Brooks et al., 2003). The lethal *cacophony* mutation is *l(1)L13*^{HC129} (Kawasaki et al., 2002). *UAS-cacophony-GFP* flies were obtained from Richard Ordway (Kawasaki et al., 2004). Animals were raised and assayed by electrophysiology as described in the text. The *w*^{1118} strain was used as a control genotype for the effects of *cacophony* mutations on synapse morphology.

Supplemental Data

The Supplemental Data for this article can be found online at http://www.neuron.org/cgi/content/full/52/4/663/DC1/.

Acknowledgments

We thank Eric Buchner for the nc82 antibody. We thank Richard Ordway for providing the *cacophony* alleles used in this study. We thank Roger Nicoll, Dion Dickman, Jan Pielage, Bruno Marie, and Kira Poskanzer for comments on an earlier version of this manuscript. This work was supported by NIH grant number NS39313 to G.W.D., an NIH NRSA to C.A.F. (NS049694), and predoctoral fellowships from NSF to C.P.G. and K.W.M.

Received: June 1, 2006
Revised: July 27, 2006
Accepted: September 14, 2006
Published: November 21, 2006

References

Albin, S.D., and Davis, G.W. (2004). Coordinating structural and functional synapse development: postsynaptic p21-activated kinase independently specifies glutamate receptor abundance and postsynaptic morphology. J. Neurosci. *24*, 6871–6879.

Atwood, H.L., Govind, C.K., and Wu, C.F. (1993). Differential ultrastructure of synaptic terminals on ventral longitudinal abdominal muscles in Drosophila larvae. J. Neurobiol. *24*, 1008–1024.

Barrett, C.F., Cao, Y.Q., and Tsien, R.W. (2005). Gating deficiency in a familial hemiplegic migraine type 1 mutant P/Q-type calcium channel. J. Biol. Chem. *280*, 24064–24071.

Beattie, E.C., Stellwagen, D., Morishita, W., Bresnahan, J.C., Ha, B.K., Von Zastrow, M., Beattie, M.S., and Malenka, R.C. (2002). Control of synaptic strength by glial TNFalpha. Science *295*, 2282–2285.

Brooks, I.M., Felling, R., Kawasaki, F., and Ordway, R.W. (2003). Genetic analysis of a synaptic calcium channel in Drosophila: intragenic modifiers of a temperature-sensitive paralytic mutant of cacophony. Genetics *164*, 163–171.

Cao, Y.Q., and Tsien, R.W. (2005). Effects of familial hemiplegic migraine type 1 mutations on neuronal P/Q-type Ca2+ channel activity and inhibitory synaptic transmission. Proc. Natl. Acad. Sci. USA *102*, 2590–2595.

Cao, Y.Q., Piedras-Renteria, E.S., Smith, G.B., Chen, G., Harata, N.C., and Tsien, R.W. (2004). Presynaptic Ca2+ channels compete for channel type-preferring slots in altered neurotransmission arising from Ca2+ channelopathy. Neuron *43*, 387–400.

Davis, G.W. (2006). Homeostatic control of neural activity: From phenomenology to molecular design. Annu. Rev. Neurosci. *29*, 307–323.

Davis, G.W., and Bezprozvanny, I. (2001). Maintaining the stability of neural function: a homeostatic hypothesis. Annu. Rev. Physiol. *63*, 847–869.

Davis, G.W., and Goodman, C.S. (1998). Synapse-specific control of synaptic efficacy at the terminals of a single neuron. Nature *392*, 82–86.

Davis, G.W., DiAntonio, A., Petersen, S.A., and Goodman, C.S. (1998). Postsynaptic PKA controls quantal size and reveals a retrograde signal that regulates presynaptic transmitter release in Drosophila. Neuron *20*, 305–315.

Dellinger, B., Felling, R., and Ordway, R.W. (2000). Genetic modifiers of the Drosophila NSF mutant, comatose, include a temperature-sensitive paralytic allele of the calcium channel alpha1-subunit gene, cacophony. Genetics *155*, 203–211.

Desai, N.S., Cudmore, R.H., Nelson, S.B., and Turrigiano, G.G. (2002). Critical periods for experience-dependent synaptic scaling in visual cortex. Nat. Neurosci. *5*, 783–789.

DiAntonio, A., Petersen, S.A., Heckmann, M., and Goodman, C.S. (1999). Glutamate receptor expression regulates quantal size and quantal content at the Drosophila neuromuscular junction. J. Neurosci. *19*, 3023–3032.

Eldefrawi, A.T., Eldefrawi, M.E., Konno, K., Mansour, N.A., Nakanishi, K., Oltz, E., and Usherwood, P.N. (1988). Structure and synthesis of a potent glutamate receptor antagonist in wasp venom. Proc. Natl. Acad. Sci. USA *85*, 4910–4913.

Evans, R.M., and Zamponi, G.W. (2006). Presynaptic Ca(2+) channels - integration centers for neuronal signaling pathways. Trends Neurosci., in press. Published online August 30, 2006. 10.1016/j.tins.2006.08.006.

Haghighi, A.P., McCabe, B.D., Fetter, R.D., Palmer, J.E., Hom, S., and Goodman, C.S. (2003). Retrograde control of synaptic transmission by postsynaptic CaMKII at the Drosophila neuromuscular junction. Neuron *39*, 255–267.

Karst, H., and Piek, T. (1991). Structure-activity relationship of philanthotoxins—II. Effects on the glutamate gated ion channels of the locust muscle fibre membrane. Comp. Biochem. Physiol. C *98*, 479–489.

Kawasaki, F., Felling, R., and Ordway, R.W. (2000). A temperature-sensitive paralytic mutant defines a primary synaptic calcium channel in Drosophila. J. Neurosci. *20*, 4885–4889.

Kawasaki, F., Collins, S.C., and Ordway, R.W. (2002). Synaptic calcium-channel function in Drosophila: analysis and transformation rescue of temperature-sensitive paralytic and lethal mutations of cacophony. J. Neurosci. *22*, 5856–5864.

Kawasaki, F., Zou, B., Xu, X., and Ordway, R.W. (2004). Active Zone localization of Presynaptic Calcium Channels Encoded by the *cacophony* locus of Drosophila. J. Neurosci. *24*, 282–285.

Macleod, G.T., Chen, L., Karunanithi, S., Peloquin, J.B., Atwood, H.L., McRory, J.E., Zamponi, G.W., and Charlton, M.P. (2006). The Drosophila cacts2 mutation reduces presynaptic calcium entry and defines an important element for CaV2.1 channel inactivation. Eur. J. Neurosci. *23*, 3230–3244.

Marder, E., and Prinz, A.A. (2002). Modeling stability in neuron and network function: the role of activity in homeostasis. Bioessays *24*, 1145–1154.

Marrus, S.B., and DiAntonio, A. (2005). Investigating the safety factor at an invertebrate neuromuscular junction. J. Neurobiol. *63*, 62–69.

McGuire, S.E., Le, P.T., Osborn, A.J., Matsumoto, K., and Davis, R.L. (2003). Spatiotemporal rescue of memory dysfunction in Drosophila. Science *302*, 1765–1768.

McKinney, R.A., Capogna, M., Durr, R., Gahwiler, B.H., and Thompson, S.M. (1999). Miniature synaptic events maintain dendritic spines via AMPA receptor activation. Nat. Neurosci. *2*, 44–49.

Murphy, T.H., Baraban, J.M., Wier, W.G., and Blatter, L.A. (1994a). Visualization of quantal synaptic transmission by dendritic calcium imaging. Science *263*, 529–532.

Murphy, T.H., Blatter, L.A., Bhat, R.V., Fiore, R.S., Wier, W.G., and Baraban, J.M. (1994b). Differential regulation of calcium/calmodulin-dependent protein kinase II and p42 MAP kinase activity by synaptic transmission. J. Neurosci. *14*, 1320–1331.

Murthy, V.N., Schikorski, T., Stevens, C.F., and Zhu, Y. (2001). Inactivity produces increases in neurotransmitter release and synapse size. Neuron *32*, 673–682.

Nicoll, R.A., and Schmitz, D. (2005). Synaptic plasticity at hippocampal mossy fibre synapses. Nat. Rev. Neurosci. *6*, 863–876.

Paradis, S., Sweeney, S.T., and Davis, G.W. (2001). Homeostatic control of presynaptic release is triggered by postsynaptic membrane depolarization. Neuron *30*, 737–749.

Perez-Otano, I., and Ehlers, M.D. (2005). Homeostatic plasticity and NMDA receptor trafficking. Trends Neurosci. *28*, 229–238.

Petersen, S.A., Fetter, R.D., Noordermeer, J.N., Goodman, C.S., and DiAntonio, A. (1997). Genetic analysis of glutamate receptors in Drosophila reveals a retrograde signal regulating presynaptic transmitter release. Neuron *19*, 1237–1248.

Piedras-Renteria, E.S., Pyle, J.L., Diehn, M., Glickfeld, L.L., Harata, N.C., Cao, Y., Kavalali, E.T., Brown, P.O., and Tsien, R.W. (2004). Presynaptic homeostasis at CNS nerve terminals compensates for lack of a key Ca2+ entry pathway. Proc. Natl. Acad. Sci. USA *101*, 3609–3614.

Plomp, J.J., van Kempen, G.T., and Molenaar, P.C. (1992). Adaptation of quantal content to decreased postsynaptic sensitivity at single endplates in alpha-bungarotoxin-treated rats. J. Physiol. *458*, 487–499.

Plomp, J.J., van Kempen, G.T., and Molenaar, P.C. (1994). The upregulation of acetylcholine release at endplates of alpha-bungarotoxin-treated rats: its dependency on calcium. J. Physiol. *478*, 125–136.

Plomp, J.J., van den Maagdenberg, A.M., Molenaar, P.C., Frants, R.R., and Ferrari, M.D. (2001). Mutant P/Q-type calcium channel electrophysiology and migraine. Curr. Opin. Investig. Drugs *2*, 1250–1260.

Rieckhof, G.E., Yoshihara, M., Guan, Z., and Littleton, J.T. (2003). Presynaptic N-type calcium channels regulate synaptic growth. J. Biol. Chem. *278*, 41099–41108.

Smith, L.A., Wang, X., Peixoto, A.A., Neumann, E.K., Hall, L.M., and Hall, J.C. (1996). A Drosophila calcium channel alpha1 subunit gene maps to a genetic locus associated with behavioral and visual defects. J. Neurosci. *16*, 7868–7879.

Smith, L.A., Peixoto, A.A., Kramer, E.M., Villella, A., and Hall, J.C. (1998). Courtship and visual defects of cacophony mutants reveal functional complexity of a calcium-channel alpha1 subunit in Drosophila. Genetics *149*, 1407–1426.

Stelling, J., Sauer, U., Szallasi, Z., Doyle, F.J., 3rd, and Doyle, J. (2004). Robustness of cellular functions. Cell *118*, 675–685.

Sutton, M.A., and Schuman, E.M. (2005). Local translational control in dendrites and its role in long-term synaptic plasticity. J. Neurobiol. *64*, 116–131.

Sutton, M.A., Wall, N.R., Aakalu, G.N., and Schuman, E.M. (2004). Regulation of dendritic protein synthesis by miniature synaptic events. Science *304*, 1979–1983.

Sutton, M.A., Ito, H.T., Cressy, P., Kempf, C., Woo, J.C., and Schuman, E.M. (2006). Miniature neurotransmission stabilizes synaptic function via tonic suppression of local dendritic protein synthesis. Cell *125*, 785–799.

Thiagarajan, T.C., Piedras-Renteria, E.S., and Tsien, R.W. (2002). alpha- and betaCaMKII. Inverse regulation by neuronal activity and opposing effects on synaptic strength. Neuron *36*, 1103–1114.

Thiagarajan, T.C., Lindskog, M., and Tsien, R.W. (2005). Adaptation to synaptic inactivity in hippocampal neurons. Neuron *47*, 725–737.

Tomancak, P., Beaton, A., Weiszmann, R., Kwan, E., Shu, S., Lewis, S.E., Richards, S., Ashburner, M., Hartenstein, V., Celniker, S.E., et al. (2002). Systematic determination of patterns of gene expression during Drosophila embryogenesis. Genome Biol. *3*, RESEARCH0088.1–88.14.

Turrigiano, G., Abbott, L.F., and Marder, E. (1994). Activity-dependent changes in the intrinsic properties of cultured neurons. Science *264*, 974–977.

Turrigiano, G.G., and Nelson, S.B. (2004). Homeostatic plasticity in the developing nervous system. Nat. Rev. Neurosci. *5*, 97–107.

Turrigiano, G.G., Leslie, K.R., Desai, N.S., Rutherford, L.C., and Nelson, S.B. (1998). Activity-dependent scaling of quantal amplitude in neocortical neurons. Nature *391*, 892–896.

Wagh, D.A., Rasse, T.M., Asan, E., Hofbauer, A., Schwenkert, I., Durrbeck, H., Buchner, S., Dabauvalle, M.C., Schmidt, M., Qin, G., et al. (2006). Bruchpilot, a protein with homology to ELKS/CAST, is required for structural integrity and function of synaptic active zones in Drosophila. Neuron *49*, 833–844.

Xing, B., Ashleigh Long, A., Harrison, D.A., and Cooper, R.L. (2005). Developmental consequences of neuromuscular junctions with reduced presynaptic calcium channel function. Synapse *57*, 132–147.